

to appear in: Comprehensive Adhesion Science, VOI II, The Mechanics of Adhesion, Rheology of Adhesives
and strength of adhesive bonds

last revised: May 10th 2001

TACK

Costantino Creton
Laboratoire PCSM
Ecole Supérieure de Physique et Chimie Industrielle
10, Rue Vauquelin
75231 Paris Cedex 05
France
Email: Costantino.Creton@espci.fr

Pascale Fabre
Centre de Recherche Paul Pascal
Av. Dr Schweitzer
33600 PESSAC
France
Email : fabre @ crpp.u-bordeaux.fr

Table of contents

| | |
|--|-----------|
| I. INTRODUCTION | 4 |
| II. EXPERIMENTAL METHODS | 4 |
| III. ANALYSIS OF THE BONDING AND DEBONDING MECHANISMS | 5 |
| III.1 Bonding process..... | 6 |
| III.2 Debonding mechanisms | 6 |
| III.2.1 Initiation of failure: Cavitation | 6 |
| III.2.2 Foam formation | 7 |
| III.2.3 Fibrillation and failure..... | 8 |
| III.2.4 Effect of geometry..... | 8 |
| IV. MOLECULAR STRUCTURE AND ADHESIVE PROPERTIES | 9 |
| IV.1. Influence of molecular parameters: nature of the monomers | 10 |
| IV.1.1. Glass transition temperature T_g | 10 |
| IV.1.2. Monomer polarity..... | 11 |
| IV.2. Influence of molecular parameters : characteristics of the chain..... | 11 |
| IV.2.1. Molecular weight of the chain M_n | 11 |
| IV.2.2. Molecular weight between entanglements M_e | 12 |
| IV.2.3. Chemical crosslinks and molecular weight between crosslinks M_c | 12 |
| IV.3. Influence of the organization of the chains at a nanometric scale | 13 |
| IV.3.1. Block copolymers..... | 13 |
| IV.3.2. Change in structure through phase transition | 14 |
| IV.3.3. Heterogeneous particles | 15 |
| IV.4. Role of other components | 15 |
| IV.4.1. Tackifiers | 15 |
| IV.4.2. Surfactants | 16 |
| V. INFLUENCE OF EXPERIMENTAL PARAMETERS | 16 |
| V.1. Velocity, temperature, time and pressure of contact | 16 |
| V.1.1. Time-temperature superposition principle..... | 16 |
| V.1.2. Effect of changing the temperature | 17 |
| V.1.3. Effect of changing the debonding velocity: cohesive to adhesive transition..... | 17 |
| V.1.4. Role of contact time and pressure..... | 18 |
| VI. SURFACE EFFECTS..... | 20 |
| VI.1. Adhesion on low G_c surfaces..... | 20 |
| VI.2. Effect of surface roughness | 21 |
| VII. CONCLUSIONS | 22 |

VIII. FURTHER READING 23

IX. REFERENCES 23

I. INTRODUCTION

In order to be effective, an adhesive must possess both liquid properties, to wet the surface when the bond is formed, and solid properties, to sustain a certain level of stress during the process of debonding. Structural adhesives accomplish this by a chemical reaction, typically a polymerization, which transforms a liquid mixture of oligomers into a crosslinked polymer. For pressure-sensitive adhesives (PSA) however this transition must occur without any change in temperature or chemical reaction. This property is called tack and gives PSA the ability to form a bond of measurable strength by simple contact with a surface. It gives PSA their easy and safe handling, since the adhesive can be applied to the surface without the use of any solvent, dispersant or heat source.

Since a PSA must have some amount of tack to be considered as such, it is essential to understand what are the minimum requirements in terms of molecular structure of the components and in terms of formulation for a material to be tacky. However, because tackiness is a complex and not yet completely understood mechanism, it is relatively difficult to establish simple relevant criteria for a good adhesive material.

Traditionally, tack properties of a PSA have been correlated to their linear rheological behavior, such as elastic and loss modulus¹⁻³. While this type of phenomenological analysis provides many clues for the practical design of PSA, it is intrinsically limited by the fact that a tack experiment involves large strains and transient behaviors of the PSA, which cannot be easily predicted by either viscosity (shear, elongational) or any other small strain steady-state dynamical property. The simple observation of the debonding of a PSA tape from a solid reflects the complexity of the phenomena at work : final rupture often occurs through the formation of a fibrillar structure^{4,5} and measured tack energies are much larger than the thermodynamic work of adhesion W_a characterizing the reversible formation of chemical bonds at the interface.

Moreover, to consider the adhesive alone is not sufficient to predict its behavior in a situation where surface effects can be important : the occurrence of bubbles or fibrils is not only a matter of the viscoelastic properties of the adhesive but depends also on the characteristics of the surface of the adherent : roughness, surface tension, and on the thickness of the adhesive film. In fact, surface and bulk effects are coupled and it would thus be more accurate to consider adhesive/substrate pairs than adhesives and substrates separately.

Despite these difficulties, recent experimental and theoretical work focusing on the microscopic

mechanisms taking place during the debonding of the PSA from the substrate, have greatly enhanced our understanding of tackiness.

II. EXPERIMENTAL METHODS

Since by definition a tacky material must be sticky to the touch, all standardized testing methods of tackiness seek to reproduce in one way or another the test of a thumb being brought in contact and subsequently removed from the adhesive surface. The main experimental methods to quantify tack can be divided into two categories: methods which provide essentially a single number are designed to be very close to the application and mainly aimed at quick comparisons between materials. Among those, described schematically on figure 1, are loop tack, rolling ball or rolling cylinder tack. In those methods, typically the contact time, debonding velocity, applied pressure, are reasonably reproducible but cannot be independently controlled. At the other extreme, probe methods are more difficult to implement (although standard instruments are commercially available) but provide much more information and allow the control of the main experimental parameters independently. Because these tests are more informative they will be the focus of the rest of this paper.

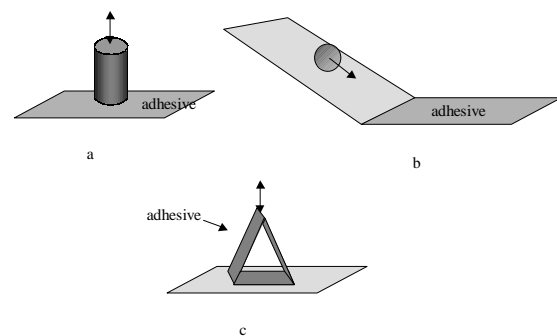


Figure 1: Schematic of the different methods for the evaluation of tack properties. a) probe tack ; b) rolling ball tack, c) loop tack

All probe methods are based on the physical principle described on figure 2. A probe, with a flat or spherical tip, is brought in contact with the adhesive film, kept in contact for a given time and under a given average compressive pressure, and then removed at a constant velocity V_{deb} . The result of the test is a force vs. displacement curve of the adhesive film in tension.

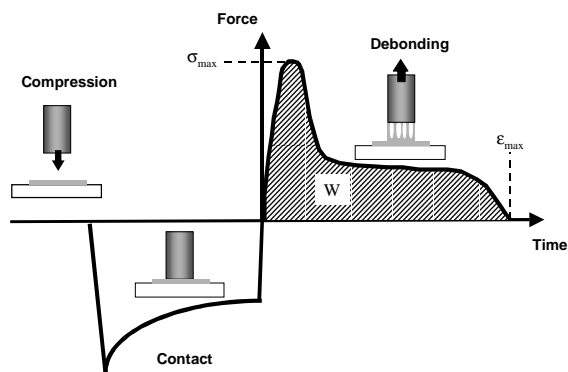


Figure 2: Schematic of a probe tack test

Several variations of the test exist. Historically, the first referenced probe test is the Polyken probe tack test developed by Hammond⁶. In this case the probe has a flat tip and is upside down. The compressive force is controlled by lifting a weight over which the adhesive is deposited. In this early version, only the maximum force of the debonding curve was recorded and taken as a measure of tack. An improvement over this methodology was developed by Zosel⁷, who used a displacement controlled instrument and pointed out the importance of considering the complete debonding curve rather than simply the maximum in tensile force. He also used for the first time in-situ optical observations during the debonding of the probe, demonstrating that good adhesives are able to form bridging fibrils between the probe and the substrate⁴. However it is only recently that the sequence of microscopic processes occurring during the debonding of a flat-ended probe from a soft adhesive were elucidated, again thanks to in-situ optical observations and measurements^{8,9}. In parallel to this development, other groups have been using spherical tip probes to test tackiness. Using a spherical tip has two important consequences. It solves the practical problem of good alignment between the probe and the film which gave rise to poor reproducibility of the results¹⁰ and it allows, at least in the early stages of the debonding process, to study quantitatively the motion of a circular crack and to use the energy release rate concepts at the edge of the contact zone¹¹ to measure a value of G_c , the critical energy release rate. However, this latter approach, often called the JKR method, is limited to relatively elastic PSA as discussed in detail in chapter X of this book. For soft and highly viscoelastic systems, using a flat probe has the advantage of applying a uniform displacement field to the layer facilitating the analysis of the fibrillation process. This chapter will therefore focus on results obtained with the flat probe with a particular emphasis on the

recent theoretical and experimental developments which have shed some light on the microscopic mechanisms of debonding.

III. ANALYSIS OF THE BONDING AND DEBONDING MECHANISMS

The tackiness of a specific adhesive is dependent on its ability to bond under light pressure and short contact time, while forming a fibrillar structure upon debonding from the substrate. It is then natural to test tackiness with a quick bonding and debonding test such as those described in the introduction.

Unfortunately such a test applies a rather complicated loading and unloading cycle to a highly deformable material. Therefore, a microscopic analysis of the sequence of events occurring during a tack test is necessary in order to attempt a detailed interpretation of a tack curve. Rather than presenting an exhaustive review of the most recent theories, we have chosen to present here a rather phenomenological picture which, while it leaves certain aspects unexplained, remains consistent with experimental results.

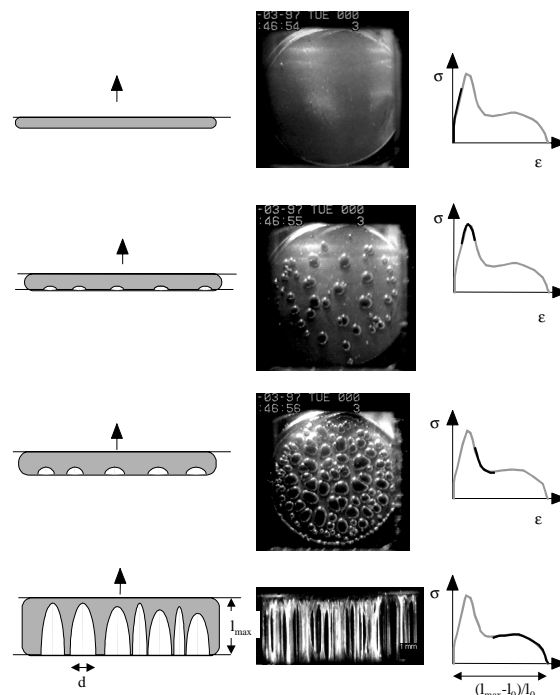


Figure 3: Schematic of the deformation mechanisms taking place during a probe tack test and corresponding images of the stages of debonding. Images from ¹².

Starting from a flat probe tack test such as that described on figure 2, the sequence of events can be broken down into four main events⁸:

Bonding to the surface of the adherent
(compression)

First stage of debonding : Initiation of the failure process through the formation of cavities or cracks at the interface or in the bulk (tension, small deformation)

Second stage of debonding : Formation of a foamed structure of cavities elongated in the direction normal to the plane of the adhesive film (tension, large deformation)

Final stage of debonding: Separation of the two surfaces either by failure of the fibrils (cohesive failure, i.e. some adhesive remains on both surfaces) or by detachment of the foot of the fibrils from the surface (adhesive failure, i.e. there is no adhesive left on the probe surface). Note that we refer here to a visually observable presence or absence of adhesive on the surface. Surface analysis techniques like XPS almost always find molecular traces of adhesive on the adherent's surface.

The debonding part of this sequence of events is shown on figure 3 in parallel with a stress-strain measurement. While the exact sequence of events depends also on the geometry of the test and thickness of the adhesive layer as discussed in section III.2.4, the general features of a stress-strain curve obtained in a probe test of a PSA, remain the same and will be characterized typically with three parameters defined on figure 2: a maximum stress σ_{max} , a maximum extension ϵ_{max} , and a work of separation W , defined as the integral under the stress-strain curve. This work of separation should not be confused with the thermodynamic work of adhesion W_a , an interfacial equilibrium parameter calculated from the values of surface and interfacial energies or with G_c , characterizing an energy dissipated during the propagation of a crack and which will be discussed in more detail in section III.2.2.

III.1 Bonding process

The requirements for a good bonding to the surface of the adherent have been discussed by Dahlquist some years ago and these requirements are still widely used in the industry today¹³. They specify that a PSA needs to have a tensile elastic modulus E' at 1 Hz lower than 0.1 MPa to bond properly to the surface. More recently this criterion has been rationalized in terms of the contact between a rough surface against an elastic plane^{14,15}. The key result of this study is that one expects a good molecular contact under zero pressure when the surface forces exactly balance the elastic energy cost involved in deforming the adhesive film to conform to the rough surface. In terms of elastic modulus of the adhesive this can be written as:

$$E < W_a \left(\frac{R^{1/2}}{\zeta^{3/2}} \right) \quad (1)$$

where R represents the average radius of curvature of the asperities of the model surface and ζ represents the average amplitude of the roughness. For $R \sim 50 \mu\text{m}$, $\zeta \sim 2 \mu\text{m}$ and $W_a \sim 50 \text{ mJ/m}^2$, one finds a threshold elastic modulus of the order of 0.1 MPa.

III.2 Debonding mechanisms

A bonding model can predict whether the bonding stage will occur properly but is not sufficient to know the level of energy dissipation which will occur upon debonding (for example water would easily pass the test but is not a useful PSA). Therefore, we will now consider the details of the debonding process.

Normally after the contact is established during the bonding stage, a tensile force is applied to the adhesive film until failure and debonding occurs. A useful PSA will require a much larger amount of mechanical work to break the contact than to form it and this work is in particular done against the deformation of bridging fibrils which can extend several times the initial thickness of the film as shown on figure 3^{4,8,16,17}.

III.2.1 Initiation of failure: Cavitation

Since the adhesive material is rubbery, it deforms at nearly constant volume and the formation of fibrils can only occur through the prior formation of voids between them. Depending on the experimental system, these voids can first appear at the interface between the adhesive and the adherent or in the bulk of the adhesive layer but they invariably expand in the bulk of the adhesive layer as illustrated on figure 3^{8,18}.

The occurrence of this cavitation process can be readily understood by noting that the elastic tensile modulus E of a typical PSA is about four to five orders of magnitude lower than its bulk compressive modulus. A mechanical analysis of the growth of an existing cavity in an elastic rubber shows that in such a medium, a preexisting cavity is predicted to grow in an unstable manner if the applied hydrostatic tensile pressure exceeds the tensile modulus E of the adhesive^{19,20}. This expansion condition can be roughly written as:

$$\sigma > E \quad (2)$$

If the nucleation of cavities is indeed responsible for the decrease in the tensile force on figure 2, according to equation 2 one expects the measured σ_{max} to be directly related to the elastic modulus E of the adhesive and therefore to obey time-temperature superposition. This is indeed confirmed by experiments showing that for several PSA on steel surfaces, σ_{max} at a given reduced debonding rate is directly proportional to E' (the value of the elastic modulus measured with steady state oscillatory shear measurements) at an equivalent reduced average deformation rate^{8,18}. This result, shown on figure 4, implies therefore that, provided that Dahlquist's criterion is satisfied, the larger the elastic modulus of the PSA, the higher its tack force on a high energy surface. This statement may however no longer be true for low energy surfaces as discussed in section VI.1.

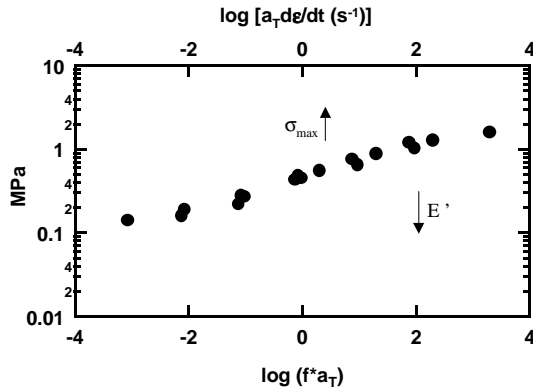


Figure 4: σ_{max} and E' as a function of the reduced shear frequency $a_T f = \omega/2\pi$, where a_T is the WLF shift factor, or of the reduced strain rate $a_T dE/dt$. (●) σ_{max} ; (---) E' . Data from ⁸.

Moreover, it should be kept in mind that such a simplistic model for the nucleation of cavities would predict a simultaneous expansion of all existing cavities at the same identical applied hydrostatic stress. This is contrary to experimental results which show that cavities appear sequentially at a range of applied stresses. Furthermore, a difficult outstanding question is that of the nature of the defects able to expand into cavities. Gay and Leibler argued that, for rough surfaces or rough adhesives, cavities should expand from defects consisting of air bubbles trapped at the interface during the bonding process¹⁶. This may be true in certain cases but cavities are just as easily nucleated on smooth surfaces and in the bulk. Better criteria for the expansion of a cavity, considering the existence of defects, are currently developed to obtain a quantitative prediction of the maximum tack stress²¹.

III.2.2 Foam formation

Until now the viscoelastic properties of the adhesive and the surface properties of the substrate (except for its roughness) have not played a significant role in controlling the mechanisms. They will be essential however in the subsequent process, i.e. the evolution of individually expanded cavities into an elongated microfoam structure. Although the formation of the foam is a rather complicated process it can be approximately characterized by two important parameters: the cell size d in the plane of the adhesive film and the maximum extension l_{max} of the cell walls in the direction normal to the plane of the adhesive film as shown on figure 3.

The final size of the cells d of the foam will clearly play a role in the macroscopic stress sustained by the walls. This final size of the cells will be controlled by three parameters which are characteristic of the behavior of the adhesive and of the interface²¹⁻²³. Two of them are bulk parameters, the unrelaxed elastic modulus of the adhesive E_o (typically at high frequency) and the average Deborah number at which the experiment is being conducted. This Deborah number is defined as the product of the initial macroscopic strain rate of the test V_{deb}/h_o , by a relevant relaxation time of the adhesive τ .

$$De = \tau V_{deb}/h_o \quad (3)$$

where h_o is the initial thickness of the film and V_{deb} is the probe velocity. At high values of De , one assumes that the adhesive behaves essentially elastically with a modulus E_o , while at low values of De , significant relaxation of the stresses can occur within the time frame of the experiment. The third parameter is interfacial: It is the critical energy release rate G_c characteristic of an adherent/adhesive pair. It can be approximately defined as:

$$G_c = G_o (1 + a_T \phi(\dot{a})) \quad (4)$$

where G_o is the energy release rate extrapolated at a vanishing crack velocity \dot{a} , a_T is the time-temperature shift factor and ϕ is a bulk dissipative function which depends on debonding rate^{24,25}. G_c characterizes the amount of energy dissipated by a propagating crack at the interface between the PSA and the surface. This parameter is widely used to characterize the adhesion between a crosslinked elastomer and a hard surface^{25,26} and, with some precautions, can also be used for viscoelastic PSA's¹¹.

Coming back to the foam formation, the simplest case is that of high values of G_c and high Deborah numbers. In this case, the characteristic lateral dimension of the cells d will only be controlled by the elastic modulus E and the thickness of the layer h_o :

$$d \approx h_o \left(\frac{K}{E} \right)^{1/2} \quad (5)$$

where K is the bulk modulus of the adhesive^{21,22}. The distance d is representative of the length over which the stress is relaxed by the expansion of the cavity. Forgetting about numerical constants, this means that one expects the lateral dimension of these cells to be directly related to the thickness of the film and inversely proportional to the square root of the shear modulus (the bulk modulus K does not vary much from one soft adhesive to another and is of the order of 1 GPa).

If the polymer can relax during the test ($De < 1$), the cavities can expand laterally causing what is analogous to a dewetting of the sample as shown on figure 5²³.

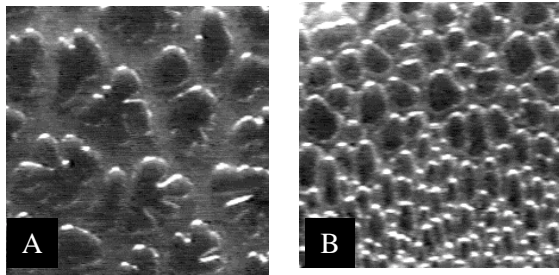


Figure 5. Comparison of the observed cavities in a poly(2-ethylhexyl acrylate) adhesive debonded : A) at 10 micrometers/s and B) at 100 micrometers/s. Images from ⁸.

III.2.3 Fibrillation and failure

Assuming that the cavities have expanded laterally as much as they can without coalescing, the last stage of the debonding process will start with the vertical elongation of the walls between cells. This mechanism implies that, at the molecular scale, there is a progressive orientation of the polymer chains in the direction of traction^{27,28}. There is an interesting analogy between this process and the formation of craze fibrils in glassy and semi-crystalline polymers. However while craze fibrils grow in length only by drawing fresh material from a reservoir of unoriented polymer²⁹, the situation is less clear for PSA fibrils where some of the extension is a result of fibril creep and some is due

to the drawing of unoriented polymer from the foot. The respective weight of these two mechanisms will depend on the rheological properties of the adhesive in elongation: a weakly strain hardening adhesive will favor fibril creep, while fibrils formed by a strongly strain-hardening adhesive will grow by drawing of unoriented polymer from the foot. Once most of the polymer chains are well-oriented, the stress on the fibrils can increase again, causing either an instability and a fracture of the fibrils themselves (macroscopically a cohesive fracture) or the detachment of the foot of the fibril from the surface of the adherent (macroscopically an adhesive fracture).

The occurrence of one or the other of these processes will depend on a delicate balance between the tensile properties of the adhesive and the interfacial parameter G_c . Despite the fact that the level of stress and the maximum extension that these fibrils will achieve often controls the amount of work necessary to debond the adhesive (the external work done during this process can sometimes represent up to 80% of the practical debonding energy), no quantitative analytical treatment of this extension and fracture process exists for such highly non linear materials. Numerical methods have however been successful in predicting at least the extensional behavior if not the point of fracture^{30,31}.

III.2.4 Effect of geometry

While the above section oversimplifies the debonding process by separating it into individual stages which are not really independent from each other, it is however a first step towards a better understanding of the critical parameters controlling tackiness. The three stages of debonding described earlier, assumed that cavitation was the first mechanism in the failure process. While this is true for useful PSA, it is worthwhile to briefly consider the limits where this may no longer be true. When a tensile stress is applied to a confined layer of arbitrary elastic modulus, one can envision two limiting cases: a very hard adhesive will not cavitate but form a crack (and the probe tack will become the butt joint geometry) and a simple liquid will form a single filament (and this experiment is called a squeeze-flow test).

In order to understand in which conditions cavitation is likely to occur, it is necessary to consider the effect of the coupling between the experimental geometry and the mechanical and interfacial properties of the adhesive on the failure mechanisms.

The results of fracture tests of adhesive bonds are almost never independent of the experimental geometry because the presence of the interface with its discontinuity in elastic properties ensures that

the stress field at the interface depends on both the external loading and the elastic properties mismatch as discussed in chapters on hard adhesives. However soft adhesives have the added complication to dissipate energy, not only in a restricted plastic zone near the interface, but over a large volume, often the entire volume of the sample. This means that there is a very strong coupling between the boundary conditions of the test (thickness of the layer, size of the probe and stiffness of the probe) and the observed deformation mechanisms.

In a recent study, Crosby et al.³² have discussed the different possible initial failure mechanisms of a thin adhesive elastic layer in a probe test and have extracted two geometrical parameters which couple with the two material parameters E and G_c : the degree of confinement of the adhesive layer (represented by the ratio of a lateral dimension over a thickness of the layer) and a characteristic ratio between the size of a preexisting internal flaw a_c and a lateral dimension of the system a . They distinguished among three main types of initial failure: bulk cavitation, internal crack and external crack as shown on figure 6.

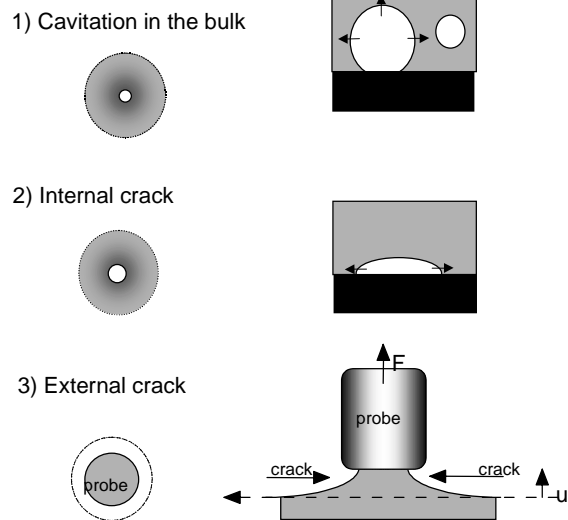


Figure 6: Schematic of the initial failure mechanisms of the elastic layer. Top views (left) and side views (right). Arrows indicate the direction of expansion of the cracks or cavities. In the case of bulk cavitation, the nucleation can be at the interface or in the bulk.

When the confinement is high, elastic instabilities such as cavitation in the layer are strongly favored, the more so of course if the elastic modulus of the adhesive is low and the interfacial energy release rate G_c is high. On the other hand, weak adhesion, a higher elastic modulus and a lesser degree of confinement all favor crack propagation as shown on figure 7.

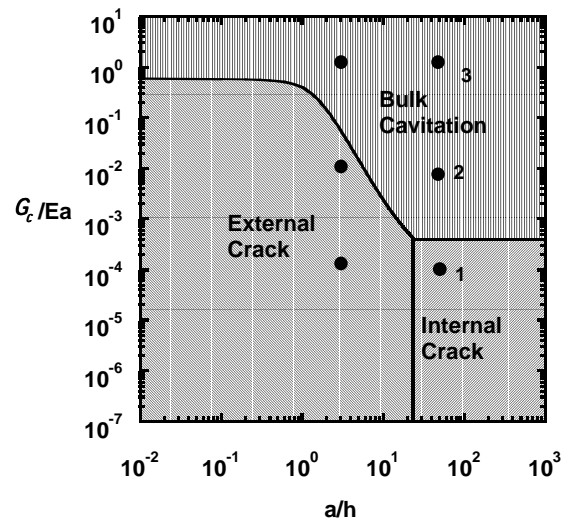


Figure 7: Deformation map with G_c/Ea as a function of a/h . Points 1 : low value of G_c/E , transition from external crack to internal crack with increasing confinement. Points 2 : intermediate value of G_c/E , transition from external crack to cavitation with increasing confinement. Points 3 : high values of G_c/E , always failure by cavitation. Case 1 is typical of a crosslinked rubber on steel or of a block copolymer-based PSA on release paper, case 2 is typical of an acrylic PSA on release paper and case 3 is typical of a PSA on high energy surfaces.

IV. MOLECULAR STRUCTURE AND ADHESIVE PROPERTIES

A polymer (or copolymer) chain is characterized by the nature and distribution of its constitutive monomers along the chain, and molecular parameters such as its number average molecular weight M_n and polydispersity M_w/M_n , its average molecular weight between entanglements M_e and its degree of branching. These factors have an important effect on the bulk properties of the material, such as the glass transition temperature T_g or the large scale organization. On the other hand, the molecular parameters also determine the rheological behavior, expressed by the different moduli and characteristic relaxation times for small (monomer) or large (chain or a part of a chain) scale motions. In Figure 8, is represented the typical tensile modulus E of a high molecular weight polymer with a narrow molecular weight distribution. At a given temperature, for relaxation times shorter than a characteristic time t_e , or frequencies of motion larger than $1/t_e$, the chain is unable to relax at a large scale : the high frequency value of the modulus is related to the nature of the monomers and their local mobility. Between t_e and

t_d , the chain is relaxed on a typical scale corresponding to the distance between entanglements : one observes a plateau region for the modulus E_o , where its value is inversely proportional to the average molecular weight between entanglements M_e . Finally, at times larger than t_d , the polymer flows like a liquid : in this range, the value of the modulus is related to the polymer molecular weight, and its degree of branching^{33,34}.

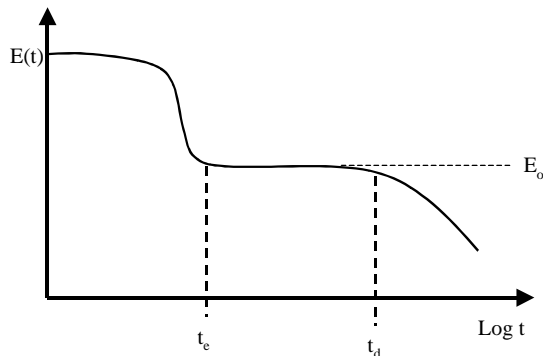


Figure 8: Relaxation modulus $E(t)$ as a function of time at a fixed temperature for a high molecular weight polymer with a narrow molecular weight distribution.

It is helpful, in order to understand the adhesive behavior of a PSA, to compare, for the same temperature, the typical experimental times or frequencies involved in a quick tack experiment (contact time, separation rate) to the characteristic relaxation times defined above. For instance, when the bond formation step is realized in a time shorter than t_e , the very high modulus of the material will prevent it from making a good contact, thus leading to a poor adhesive behavior. In a similar way, the separation rate has to be within a range where fibrils can form in order to obtain large dissipation and thus a good adhesive behavior. In practical situations the separation rate and temperature are usually imposed by the specific use that is being made of the adhesive, so that one needs to play with the molecular weight of the polymer, its degree of branching or crosslinking and the monomer friction coefficient in order to modify its relaxation times and thus its viscoelastic losses during the fibrillation stage. Thus, even if not sufficient by itself, the knowledge of the linear viscoelastic properties E' and E'' versus frequency curve gives a strong indication of the suitability of a given material for adhesive purposes.

As a first approximation, a suitable molecular structure for a tacky material could be described as a nearly uncrosslinked network : a low plateau modulus will give a high compliance of the layer and therefore a good contact with the surface, and crosslinks and entanglements will give the necessary cohesive strength to form stable fibrils at debonding frequencies. In practice, this is often

realized by combining two main ingredients: a partially crosslinked, low T_g high molecular weight component and a high T_g , low molecular weight component called a tackifier, but as we will see in the following, many types of structures can lead to the right balance of properties.

IV.1. Influence of molecular parameters: nature of the monomers

IV.1.1. Glass transition temperature T_g

Since the characteristic relaxation times of the base-polymer in the PSA are always decreasing with temperature, one would expect the properties of a PSA to be also monotonically dependent on temperature : experimentally however one observes the existence of a fairly sharp optimum of the tack properties of a material with temperature. This is illustrated in Figure 9, for various polyacrylates³⁵ and will be discussed in more detail in section V.1.2. More generally, it is admitted that, for the PSA properties of an adhesive to be optimal, its T_g should lie somewhere between 70°C and 50°C below the use temperature for an acrylate or natural rubber based adhesive and between 30 and 50°C below the usage temperature for an SBC (styrenic block copolymer) based adhesive. This temperature corresponds to a balance between an elastic modulus E lower than 10^5 Pa (Dahlquist's criterion) and a high level of dissipation upon debonding. It is in fact one of the roles of a tackifying resin, or of a comonomer in an acrylic PSA, to raise the T_g of the system when the T_g of the polymer alone is too low.

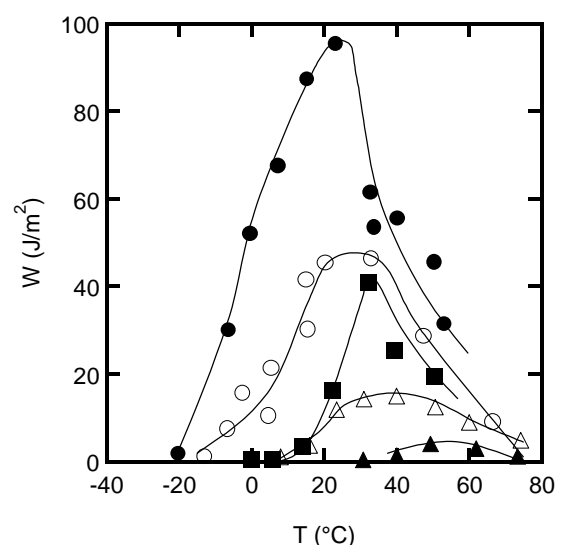


Figure 9: Debonding energy W as a function of temperature for probe tack tests of different acrylic polymers. (●) Poly(2-ethylhexyl acrylate) ; (○) Poly(n-butyl acrylate) ; (■) Poly(isobutyl acrylate) ; (△) Poly(2-ethylhexyl acrylate)

acrylate) ; (\triangle) Poly (ethyl acrylate) ; (\blacktriangle) Poly (methyl acrylate). Contact time 0.02 s. Data from 35.

IV.1.2. Monomer polarity

Since it was noticed that the incorporation of polar monomers such as acrylic acid could enhance the cohesive and adhesive strength of a material, several studies have been devoted to the role played by the polarity of the monomer in the adhesion process.

The influence of incorporating polar monomers is complex : it both modifies the surface tension and the bulk properties of the adhesive. However these two effects are not generally dominant at the same time. In tack experiments, the most visible change brought about by acrylic acid is a sharp increase in the long relaxation times of the polymer³⁶. As shown on figure 10, this causes a shift in the characteristic debonding rate at which the transition from cohesive failure of the fibril to adhesive failure is observed¹⁸.

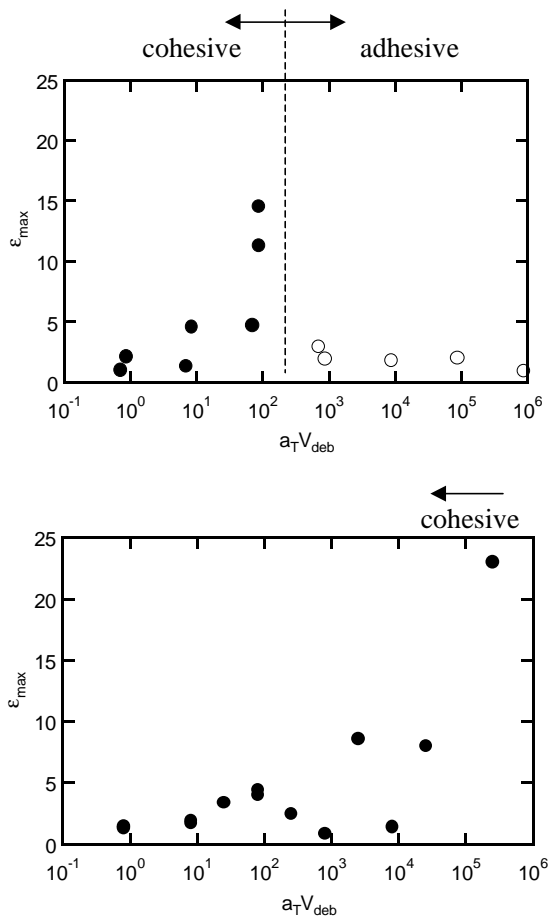


Figure 10: Maximum extension of the fibrils ϵ_{max} as a function of reduced debonding rate $a_T V_{deb}$. a) for the PnBA with 2.5% acrylic acid; b) for the PnBA without acrylic acid. $T = 23^\circ\text{C}$, $t_c = 1$ s. (\bullet)

cohesive failure ; (\circ) adhesive failure. Data from 18.

However in peel tests, which typically involve long contact times, the dominant effect is reversed: acrylic acid moieties can slowly migrate to the interface with the substrate and cause a significant increase of the interactions which can switch the fracture mode back to cohesive³⁷. More generally, the presence of monomers of different polarities can lead to specific time-dependent effects related to the kinetics of diffusion or reorientation of the different species at the surface during the experimental time. Finally, the presence of acrylic acid can suppress the time-temperature equivalence generally observed for adhesive tests of soft polymers^{8,38}.

IV.2. Influence of molecular parameters : characteristics of the chain

IV.2.1. Molecular weight of the chain M_n

Commercial PSA's have typically a very broad molecular weight distribution or alternatively a very broad distribution of terminal relaxation times. This polydispersity is essential to obtain good PSA properties.

In order to understand why this is the case, it is useful to examine the results obtained with polymers with a narrow or very narrow molecular weight distribution^{18,35,39}.

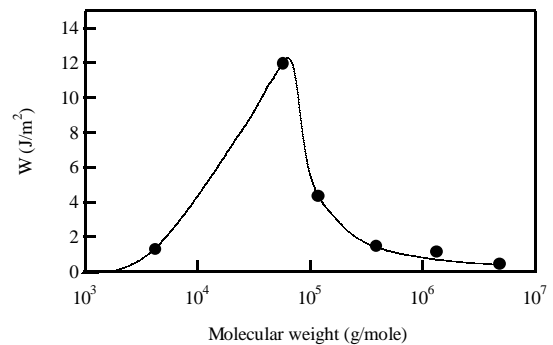


Figure 11: Adhesion energy W as a function of the weight average molecular weight for a polyisobutylene with a low polydispersity. Data from 35.

As shown on figure 11 for a polyisobutylene, if the comparison is made for the same experimental conditions, reasonable tackiness is only obtained in a relatively narrow range of molecular weights. This can be understood in the following way: the

increase of M_n increases the viscosity η , since $\eta \propto M_n^{3,4}$, or, in terms of characteristic relaxation times, the terminal relaxation time τ_d . In a tack experiment, this increase in viscosity leads to a larger cohesive strength of the material, which in turn causes a better stability of the PSA fibrils, once they are fully formed, and thus to a larger value of ϵ_{max} . On the other hand, the formation of the fibrils from the initially formed cavities requires a certain amount of flow so if the terminal relaxation time and the viscosity increase too much the fibrillar structure is never formed. As a general guide, experiments conducted at room temperature and relatively high debonding rates show a maximum tack energy at a molecular weight which is approximately 5-10 times the average molecular weight between entanglements M_e .

When considering the molecular weight effects, one should nevertheless remember the influence of experimental parameters : the optimum molecular weight will depend strongly on the rate and temperature of the test with high temperatures and low debonding rates shifting the optimum towards higher molecular weights¹⁸.

Conversely, the temperature window of optimum tack for a given molecular weight will be rather narrow (approximately two decades in frequency or 10°C based on figure 10). For the more common case of polymers which are not monodisperse but have a broad molecular weight distribution, the resulting broad distribution of terminal relaxation times circumvents this problem allowing both fibril formation and fibril stability for a range of experimental conditions. As a result, an optimum in tack energy with M_n is still observed but becomes also broader and is shifted to higher molecular weights relative to the monodisperse case.

IV.2.2. Molecular weight between entanglements M_e

Entanglements are crucial in the behavior of PSA. Clearly unentangled polymers do not work well as PSA since they do not have enough cohesive strength to form stable fibrils. On the other hand the terminal relaxation time of an entangled polymer τ_d is dependent on $(M_n/M_e)^3$ from the reptation model and plays a role in controlling the elongation of the fibrils as described in the preceding section. Additionally, the average molecular weight between entanglements plays also a major role in the early stages of the debonding process since it controls the elastic modulus in the plateau region. Indeed, since tack tests are usually conducted in a frequency range where E is in its plateau region (where $E' = E_0 \propto 1/M_e$) a change in M_e has a direct consequence on the value of E' at the debonding frequency.

For polymers with molecular weights much larger than M_e , a transition in debonding mechanism is observed for M_e larger than approximately 10^4 g/mol⁴⁰. At low values of M_e , adhesive failure by crack propagation is observed while for high M_e polymers, failure by cavitation and fibrillation is observed. This transition can be understood by a purely mechanical argument. The critical stress for cavitation in the bulk to occur is proportional to the elastic modulus E' of the polymer at the testing frequency. Therefore, when E' decreases, the critical stress for cavitation decreases, and becomes eventually smaller than the G_c for crack propagation at the interface^{32 41}. Therefore, for low M_e , the initial debonding is by crack propagation and cannot then evolve towards a fibrillar structure while for high M_e , the debonding occurs through cavitation and fibrillation and a larger amount of energy is dissipated in the process. This transition from fibrillation to homogeneous deformation, which can also be concomitant with a transition from cohesive to adhesive failure, is normally accompanied by a drop in tack energy. Zosel pointed out that this critical value of M_e corresponds in fact to the Dahlquist criterion for the elastic modulus E , below which a material is not considered tacky : $E=10^5$ Pa. M_e plays thus a very important role on the debonding stage in a PSA, since it influences the ability for fibrillation, the type of rupture, and consequently the debonding energy.

IV.2.3. Chemical crosslinks and molecular weight between crosslinks M_c

Experiments on a series of PDMS adhesives, have shown that the tack energy is maximum, for a degree of crosslinking which is slightly above the gel point⁴². Below the gel point, the crosslinks' main effect is to increase the terminal relaxation time of the polymer. The presence of long branches will in particular play a large role on the elongational flow properties of the polymer and increase fibril stability. This will lead in turn to a higher value of ϵ_{max} and a higher tack energy. Above the gel point, additional crosslinking will initially have an effect on the strain hardening which occurs in extension. Significant strain hardening in extension will occur in the polymer for an increasingly lower level of strain, causing early detachment of the fibrils and a lower measured ϵ_{max} . This effect is illustrated on figure 12 on a series of acrylic polymers crosslinked beyond the gel point⁴⁰. One should note that the peak, and the height of the plateau, remain unchanged implying that the viscous dissipation in the fibrils and the plateau modulus E_0 are much less affected by a modification of the crosslink structure. By

extrapolating these measurements, one can argue that fibrillation should be suppressed altogether when the crosslink density becomes equal to the entanglement density. Following the map of figure 6, a change in mechanism from cavitation to crack propagation has occurred, mainly caused by a decrease in the interfacial dissipative term G_c this time.

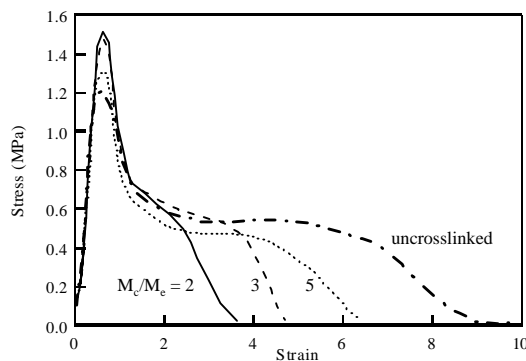


Figure 12: Stress-strain curves of PnBA on steel, UV crosslinked to different degrees as indicated by the ratio M_c/M_e . Data from ⁴⁰.

Therefore, in a similar way as entanglements do, crosslinks decrease the ability of the material to flow, and eventually lead to a transition to failure by crack propagation and coalescence, and thus to a lower tack energy. However, crosslinks are permanent and completely prevent large deformations; this is not the case for entanglements, provided that the deformation occurs at sufficiently low rates.

Crosslinking is widely used in the PSA industry to tune the properties of removable adhesives by reducing ϵ_{max} . An example of that type of effect, is the development of PSA for trauma free removal patches, where in-situ irradiation leads to crosslinking, and thus to highly reduced peeling forces for the adhesive⁴³.

IV.3. Influence of the organization of the chains at a nanometric scale

The main polymers used as PSA can be divided in a few large classes according to their chemical structures : natural rubber based, styrenic block copolymer based (mainly triblocks and diblocks of styrene and butadiene or isoprene), acrylics and for a smaller part, silicones. From a microstructural point of view, however, the classification should be different. As already mentioned, a pressure-sensitive-adhesive requires both a good shear resistance and some capability to flow in order to function properly. The resistance to shear is normally achieved by introducing crosslinks:

chemical ones as in natural rubber or acrylics, but also physical ones. In the case of strongly immiscible comonomers, for example, and depending on the chain statistics, the architecture and monomer composition of the polymer chain can lead to microphase separation so that the microscopic domains act as physical crosslinks for the system : this is the case for styrenic block copolymers. In certain cases, in addition, there can be a long range ordered structure, such as a lamellar stacking. All these structures lead to different behaviors as far as tack is concerned. We list below several types of systems, as examples of different types of phase separated structures, although their importance from an industrial point of view is not necessarily comparable.

IV.3.1. Block copolymers

Block copolymers with incompatible blocks which are able to microphase separate are good candidates for PSA properties. Indeed, blends of ABA triblocks and AB diblocks, where the rubbery midblock of the ABA is the majority phase and the glassy endblocks self organize in hard spherical domains and form physical crosslinks, are widely used as base polymers for PSA. The actual adhesives are always compounded with a low molecular weight tackifier resin able to swell the rubbery phase and dilute the entanglement network. Linear styrene-rubber-styrene copolymers, with rubber being isoprene, butadiene, ethylene/propylene or ethylene/butylene, are the most widely used block copolymers in this category.

This class of PSA has unique properties which are related to their molecular superstructure. Indeed, compared to chemical crosslinks, physical crosslinks present several advantages, the first one being that they are reversible with temperature, thus leading to a large viscosity decrease above the glass transition temperature of the endblocks : this makes these systems very suitable for hot melt processing, an increasingly popular processing method due to environmental regulations. A second advantage is that the crosslink density is naturally fixed by the composition of the system, provided that it is at equilibrium, and thus easier to control than chemical crosslinking. Finally, the physical crosslinks provided by the hard domains are quite fixed under low stresses, giving very good creep properties, but can be broken and reformed at high stresses, which is essential for the formation of the fibrillar structure.

As shown schematically on figure 13, one can distinguish two types of configuration for the triblock molecules: if the two endblocks of a molecule are incorporated in separate hard domains, the triblock will be described as a bridge.

If alternatively both endblocks are incorporated in the same hard domain, the triblock will be described as a hairpin molecule.

Although this process is not fully understood, it is believed that the number of bridge molecules between hard domains controls the large strain behavior. An increase in the amount of tackifying resin in a pure triblock copolymer causes a change in the ratio of bridge to hairpin molecules, and consequently a change in the value of ϵ_{max} as shown on figure 14.

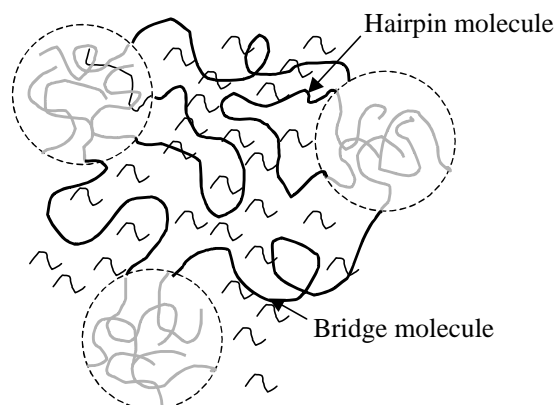


Figure 13: Schematic of the molecular structure of styrenic block copolymers showing the hairpin and bridge configurations.

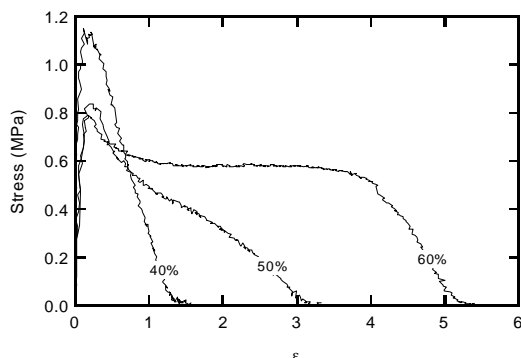


Figure 14: Stress-strain curves of an SIS + resin PSA on steel⁴⁴ with three different amounts of resin in wt%. The base polymer was Vector 4311 (Exxon) and the resin was Regalite R101 (Hercules). $V_{deb} = 10 \mu\text{m/s}$, $T = 40^\circ\text{C}$.

Similarly to the case of simpler homogeneous systems discussed in section IV.2 the rheological properties of these PSA will be essential in controlling their adhesive behavior. However the modifications of molecular structure to obtain these rheological properties will be different. For example the apparent plateau modulus E' will no longer be controlled by M_e , but by the molecular weight of the elastomeric midblock and by the amount of resin which is incorporated. The terminal

relaxation time controlling fibril extension can be somewhat tuned by replacing some of the triblock in the adhesive by double the amount of diblock with one half the molecular weight, effectively modifying the ratio of hairpin to bridges. It is important to note that this ratio can effectively be modified by the processing conditions (hot-melt, solution cast). In a recent work, Flanigan et al⁴⁵ showed that the adhesive properties of acrylic triblock copolymers cast from two different solvents could be very different, even though their structure as determined by X-ray scattering was the same, i.e. the hard domains size and spacing were identical.

Other studies on the properties of block copolymers with more complicated architectures exist although not all of them consider tack. Some studies comparing properties of radial versus simple block architecture allow to compare the effect of chemical versus physical crosslinks in the case of structured systems. The data shows that there is a decrease of melt viscosity together with better adhesive properties for star copolymers⁴⁶. This is related to a point that was discussed earlier : the different architectures of the molecules lead to different physical crosslinking densities. In the same spirit, block copolymers with four different arms, two polyisoprene, and two polystyrene-b-poly(ethylene/butylene) arms were studied, and led to a better combination of shear strength and melt viscosity for adhesive applications⁴⁷, compared to the conventional linear SIS and SEBS triblocks.

IV.3.2. Change in structure through phase transition

Previously discussed systems are always phase-separated at application temperatures and undergo a change in properties at high temperatures from elastomeric tacky to liquid for processing reasons : this change occurs over a wide temperature range. It is however possible to tune the molecular structure to obtain a transition from solid non-tacky to elastomeric tacky for a given temperature independent of debonding rate, by using a thermodynamic phase transition.

Recent experiments⁴⁸ have compared the tack properties of a given system below and above the phase transition between an organized smectic phase and an isotropic phase. The system used was a side-chain fluorinated copolymer, with two types of pendant groups both able to crystallize. Below the transition, in the smectic phase, the system possesses no tack due to its high elastic modulus that prevents the formation of a good bond with the surface. Above the transition, a soft, phase separated region with possibly a continuous network of crystalline domains, allows the system

both to achieve a good bond for short contact times and extended cavitation followed by large deformations. This type of system presents the interesting feature to have a very abrupt non tacky-tacky transition at a temperature which can in principle be varied at will by changing their monomer composition.

IV.3.3. Heterogeneous particles

There are very few studies published on PSA films obtained from heterogeneous latexes: indeed, most PSA used in the form of latexes, such as styrene-butadiene or acrylic systems, are random copolymers. Although emulsion polymerization does not allow in general as much control over the molecular structure and therefore over adhesive properties, the use of solvent-free adhesives to replace their solvent-based counterparts is increasingly important, due to the recent environmental regulations. One example where the structure of the final adhesive film can be finely tuned at a scale of a few tenths of a nanometer is given by a recent study⁴⁹ which compares the tack properties of two acrylate copolymer samples synthesized either with a batch or continuous feed process, leading to particles of different heterogeneities. The tack properties of the two systems are markedly different, thus rising the question of the role of structural heterogeneities at the particle scale. Such heterogeneities may, in principle, be probed by AFM methods, effectively performing a “nano-tack” experiment on isolated particles or on monolayers of latex particles⁵⁰: this powerful tool could help to understand the correlation between the macroscopic properties of an adhesive and its microscopic response.

IV.4. Role of other components

A formulated adhesive contains in general, in addition to the base polymer, some small molecule additives: a tackifier, and some fillers, plasticizers and antioxidants. Additionally if the adhesive has been obtained by emulsion polymerization it contains some surfactants. Tackifiers and plasticizers are added to tune the viscoelastic properties of the adhesive, while surfactants are generally unwanted residues of the polymerization process. Again, much technology, most of it proprietary, is involved in these formulation parameters and we only address here some generic points based on what is available in the open literature.

IV.4.1. Tackifiers

The role of the tackifier is to adjust the viscoelastic properties of the system. It typically consists in short chain polymers of molecular mass between 300 and 3000 g/mole, with a softening temperature between 60°C and 115°C, depending on the adhesive. The tackifying resin has a dual role: increasing the T_g of the system, which increases the viscoelastic losses at high frequencies, and decreasing the modulus at the low frequencies that are important at the bond formation stage^{51,52}. The decrease in elastic modulus in the plateau region can be interpreted as a dilution of the entanglement structure. For a given T_g of the tackifier, there is an optimum weight fraction in a PSA: at low tackifier contents, the plateau modulus is too high to satisfy Dahlquist's criterion and at high tackifier contents, the T_g of the PSA becomes too high and again poor bonding occurs.

A simple way to determine the optimum amount of resin is to determine the amount which gives the minimum value of the elastic modulus of the system as shown on figure 15³⁵.

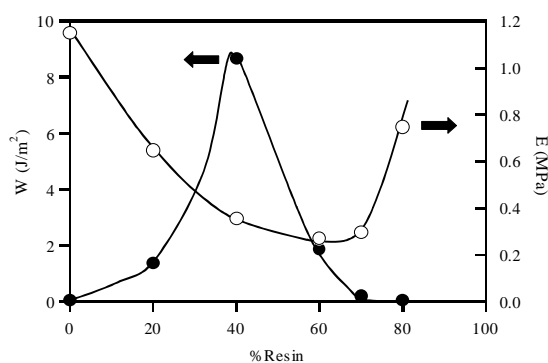


Figure 15 : Elastic modulus E in a relaxation experiment (○) and adhesion energy W in a probe tack test on steel (●) as a function of resin content for a natural rubber/glycerol ester of hydrogenated resin blend. Data from ³⁵.

Of course, in order to be able to modify the viscoelastic properties of a system, and to change the entanglement density, a tackifier needs to be miscible with the adhesive, which implies that it has to be chemically adapted to the adhesive⁵²⁻⁵⁶. This is realized via different families of tackifiers, depending on the nature of the adhesive compound. Giving an exhaustive list of tackifiers together with their compatibilities with adhesives would be beyond the scope of this review, since new families of tackifiers with better compatibility appear on a regular basis⁵⁷ but the interested reader can refer to more technologically oriented texts for further information⁵⁸.

IV.4.2. Surfactants

For emulsion adhesives, the presence and nature of surfactants is also an important parameter. Their action is twofold: by diffusing to the surface of the film, they may change its properties and its ability to form a good contact, and by plasticizing the polymer they can change its bulk properties. However while some studies have appeared on their effect on peel properties^{59,60}, not much is known on their influence on tack.

V. INFLUENCE OF EXPERIMENTAL PARAMETERS

V.1. Velocity, temperature, time and pressure of contact

In a probe tack test, several experimental parameters can be varied independently, such as the pressure p exerted by the probe on the surface of the adhesive during the compressive stage, the duration of the contact stage called contact time t_c , or the separation rate of the probe V_{deb} . Since a change in experimental parameters can sometimes lead to a change in fracture mechanism, the evolution of the adhesion energy with these parameters is in general complex, and deserves to be described a little further. When the debonding rate V_{deb} is varied, the characteristic strain rates applied to the adhesive layer are changed accordingly, which in turn modifies its viscoelastic response. The response of the material, which depends on its spectrum of relaxation times, is also a function of the temperature of the sample. The contact time t_c and pressure p can control the size of the real contact area, but also the degree of relaxation of the adhesive when the debonding starts. Effectively, this means that the initial condition of the debonding part of the test will depend on the applied pressure and contact time in the compressive part of the test. Depending on the bulk properties of the material, or on the features of the probe-adhesive interface such as roughness, this difference in initial condition can have a negligible effect (typically for soft PSA on smooth surfaces) or a large one (for stiffer PSA on rough surfaces).

V.1.1. Time-temperature superposition principle

The time-temperature (t-T) superposition principle is based on the idea that when a polymer is deformed, a change in the characteristic

deformation rate is equivalent to a change in temperature. In the context of tack tests, one can assume that the characteristic deformation rate is the V_{deb}/h_0 so that an increase in V_{deb} would be equivalent for example to a decrease in temperature. This t-T superposition, which is very widely used in linear rheology³³ where small deformations are applied, can apparently also be used for the large deformations typical of tack experiments³⁵. However a necessary condition for this t-T equivalence to apply is that no change in fracture mechanism should be induced by a change in the initial condition of the test as defined in V.1. If this change in initial condition causes a qualitative change in the mechanisms involved in the debonding stage at the microscopic level, the rate dependence of the adhesion energy has no reason to follow the t-T principle. As an example shown on figure 16, a series of tack experiments⁸ at a contact time of 60 seconds obey very well the t-T superposition while the same series of experiments at a contact time of 1 second does not. In this case, the short contact time did not allow the full relaxation of the adhesive at the lower temperature, causing therefore a change in the initial condition. Experimentally this change had a moderate effect on the cavitation process, but triggered a significant change in the later stage fibril formation process as shown on figure 16. Consequently, a master curve for σ_{max} could be easily built but not so for W as shown on figure 16b and c. This type of effect is more dominant when the surface is rough and the time of contact does not allow the adhesive to fully relax.

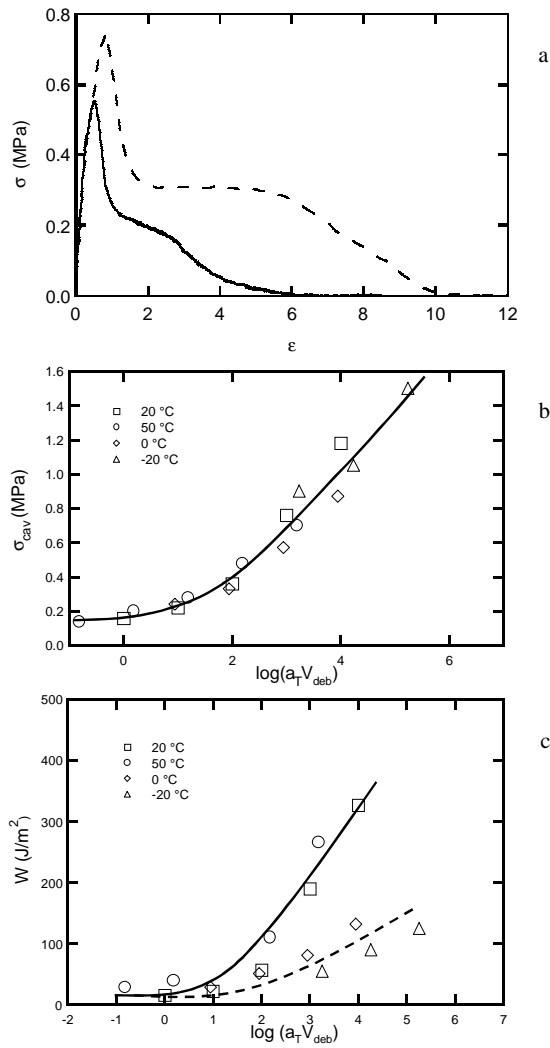


Figure 16: a) Stress-strain curves of an acrylate adhesive on steel at two identical values of reduced debonding velocity. (----) $V_{deb} = 100 \mu\text{m/s}$, $T = 0^\circ\text{C}$; (- - -) $V_{deb} = 1000 \mu\text{m/s}$, $T = 20^\circ\text{C}$. b) Maximum stress σ_{max} vs. reduced debonding rate and, c) adhesion energy W vs. reduced debonding rate for the same adhesive. Note that the low temperature data for W do not follow t - T superposition. Data from ⁸.

Another interesting example where t - T superposition fails is that of a change of temperature leading to a thermodynamic phase transition in the material (melting of a crystalline phase) and therefore to a change of structure⁴⁸. In both examples, an experimental parameter has caused a change in the *initial* condition of the debonding test which, in turn, modified the microscopic separation mechanisms.

V.1.2. Effect of changing the temperature

As explained earlier, the temperature of the test is important since it modifies the relaxation times of the polymer and therefore the rheological behavior of the material: an increase of temperature near the T_g of the polymer decreases its elastic modulus, thus leading to a better contact area and a larger adhesion energy. On the other hand, when temperature is too high, the viscosity of the system becomes very low, decreasing the adhesion energy again. Therefore a maximum in tack as a function of temperature is usually observed at approximately $T_g + 50^\circ\text{C}$ as described earlier and shown on figure 17. Although a proper formulation can extend the useful temperature range of a PSA or modify the temperature difference between the T_g and the maximum tack, it is extremely difficult to obtain a material which retains tackiness over a temperature range in excess of 50°C .

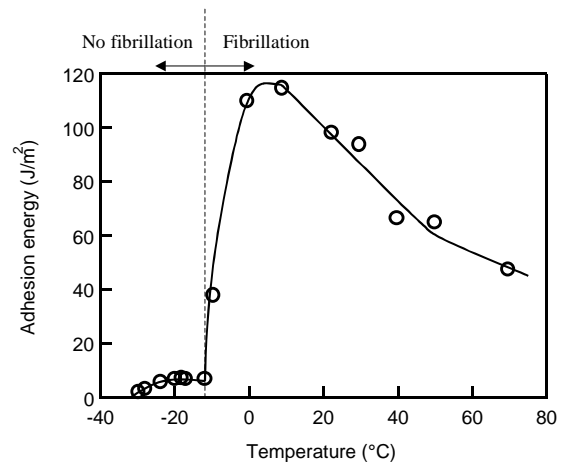


Figure 17: Adhesion energy W as a function of temperature for a PEHA adhesive on steel. The final separation is always interfacial but a clear transition between non-fibrillar and fibrillar debonding is observed at $T = -10^\circ\text{C}$. The glass transition of the adhesive is around -55°C . Data from³⁵

A more subtle effect of temperature is also displayed on figure 17 where experiments³⁵ show a rapid increase of the adhesion energy with temperature, related to a change in the rupture mechanism from interfacial fracture by crack propagation to failure by fibrillation and debonding of the fibrils. The interpretation of the authors is that the temperature change is responsible for a modification of the adhesive-probe contact area, which in turn results into different types of rupture mechanisms in the two temperature ranges.

V.1.3. Effect of changing the debonding velocity: cohesive to adhesive transition

The strain rate of an adhesive sample in a probe-tack test is related to the debonding velocity of the probe, however not in a straightforward way. Indeed, the separation stage induces very heterogeneous shear and elongation flows in the sample³². A common approximation, bypassing all these considerations, is however to consider that, at the beginning of the separation process at least, the sample is homogeneously deformed at a frequency close to V_{deb}/h_o , where h_o is the sample thickness. For a monodisperse linear polymer with well-defined relaxation times, its response can be well predicted by a Deborah number¹⁸. In the regime of cohesive failure (low De), the adhesion energy W is controlled by the value of ϵ_{max} which continuously increases with De . In this regime σ_{max} does not vary much with De . On the other hand, in the regime of adhesive failure (high De), ϵ_{max} is always low and W is mainly controlled by σ_{max} which increases with De .

In this case, a sharp drop of tack energy occurs at the transition from cohesive to adhesive failure, i.e. for $De = \tau V_{deb}/h$ between 100 and 1000. Such a transition is completely analogous to that observed by others in peel tests^{61,62} and corresponds to a change in the *initiation* mechanism of failure as discussed in section III.2.4.

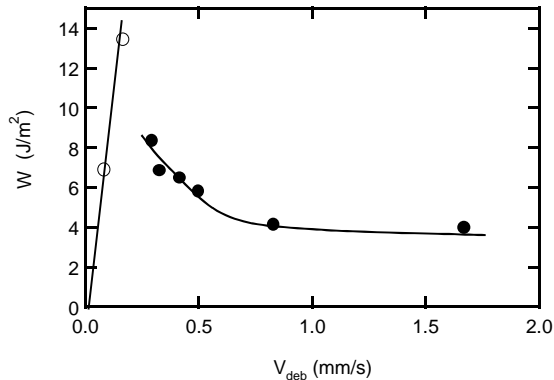


Figure 18: Adhesion energy W as a function of V_{deb} for a spherical glass indenter (JKR geometry) on a high molecular weight PDMS polymer melt. (○) cohesive fibrillar fracture ; (●) adhesive fracture. Data from ⁶³.

A similar change in mechanism with increasing velocity occurs for the debonding of a glass spherical indenter from a high-molecular weight polydimethylsiloxane (PDMS). In this case the debonding occurs in a situation of low confinement (value of a/h is low) with no cavitation. As shown in figure 18⁶³, the adhesion energy is increasing with velocity in the cohesive regime, where the separation occurs by bulk yielding and through eventual rupture of a single large column of polymer. If V_{deb} is further increased, adhesion energy drops abruptly then slowly decreases with

V_{deb} and reaches an asymptotic behavior. In this regime the separation occurs through the propagation of an external radial crack.

A similar behavior has been observed for acrylic systems when a flat probe was used (high value of a/h). As shown on figure 19, the adhesion energy slowly increased in the fibrillation regime, and dropped when the fibril formation was suppressed⁴⁰.

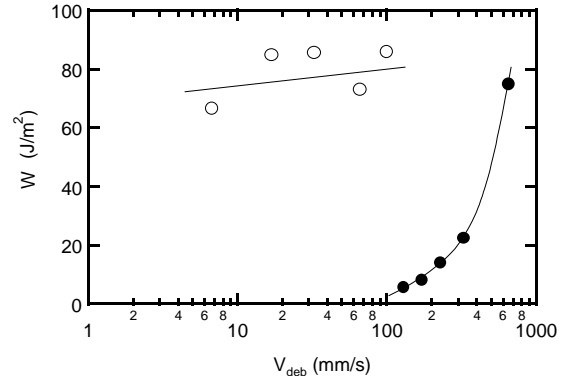


Figure 19: Adhesion energy W as a function of V_{deb} for a PEHA-based adhesive on steel at $T = 20^\circ\text{C}$ and 1 s. contact time. Transition from fibrillar (○) to non-fibrillar (●) fracture. Data from ⁴⁰.

These three experiments present two similar features : an increase of adhesion energy with V in the fibrillar regime, whether there is “one” or many fibrils, and the drop in adhesion energy when going from a fibrillar to a non-fibrillar adhesive separation process, which corresponds to a change in initial fracture mechanism from bulk yield to crack propagation. This implies that when the deformation rate is high enough to prevent significant relaxation processes in the polymer, fibril formation can be suppressed and the tack energy drops.

It should be noted that while the transition from fibrillar to non-fibrillar fracture appears to be very general, it is not necessarily concomitant with a change from cohesive to adhesive failure. It was reported to be concomitant for linear polymers¹⁸, but not for crosslinked or highly branched polymers^{8,40}.

V.1.4. Role of contact time and pressure

The adhesion energy versus contact time is plotted on figure 20a for the case of an acrylic adhesive on steel⁴⁰. The variation in W observed with increasing contact times was initially attributed to the increase of the real contact area. However more recent and more detailed results have shown that the increase in the adhesion energy was also due to a larger value of ϵ_{max} as can be seen on Fig 20b⁴⁰.

One can envision therefore two separate effects of the contact time. For very short contact times, the real area of contact may really be affected, giving therefore a lower value of σ_{max} . However for intermediate contact times, it is the fibrillation process which is mainly affected and its effect can be seen more on W than on σ_{max} .

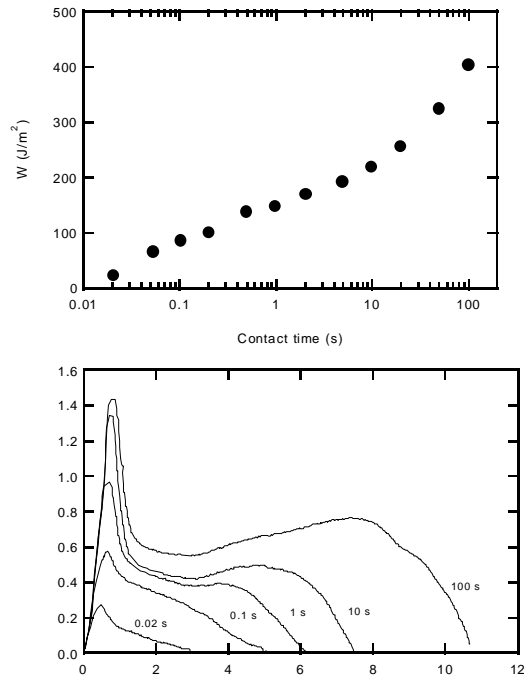


Figure 20: a) W as a function of contact time for a PnBA adhesive on steel; b) Corresponding stress-strain curves for selected contact times. Data from 40.

Presumably it is not the real contact area which is important in this case but rather the degree of relaxation of the adhesive during the contact time. If the relaxation times of the adhesive are of the same order of magnitude than the time of contact, one expects large differences in the initial stress state of the adhesive layer depending on the contact time. These differences could then lead to a different response of the adhesive during the debonding stage as shown on figure 20b. One should note that, in principle one expects W to become independent of t_c for long contact times. Although this effect has been reported³⁵, experiments do not always show a plateau within the limits of the experimentally accessible range of t_c of a few hundred seconds. Additionally, in some cases the degree of roughness of the probe may lead to trapped air and inhomogeneous stress fields which are also bound to vary with the time of contact¹⁶. Experimentally, in the regime where relaxation times of the adhesive are important, adhesion is always lower and the time of contact has always a more marked

effect for rough surfaces than for smooth ones^{40,64,65}.

In the same way and for the same reasons, a plateau in adhesion energy is observed for large contact pressures³⁵ but few systematic studies have been published for viscoelastic systems where relaxation processes during the time of contact can play a major role.

V.2. Effect of geometry

Most of the results which are discussed in this review were obtained with flat probe tack tests on thin adhesive films (20-100 μm typically). While this geometry has several advantages for the analysis of fundamental properties of PSA, it is by no means the only one that can be used and one should be careful to understand clearly what features of a tack curve are due to the material and which ones are due to the specific experimental geometry.

As discussed in section III.2.4. the experimental geometry and particularly the degree of confinement of the adhesive layer can have an important effect on the initial failure mechanisms which are observed.

Luckily for users, most PSA have properties of critical energy release rate G_c and tensile modulus E in a range which makes them relatively insensitive to the degree of confinement. Therefore tests done with spherical or flat indenters give relatively similar results.

However for very soft (liquid-like) and very hard (solid-like) PSA, testing tack with the spherical probe, which typically applies a much lesser degree of confinement to adhesive film, may lead to significantly different failure mechanisms³². Three further comments should be added concerning the role of the geometry:

The role of the geometry will be dominant only in the first stages of the debonding process since once a fibrillar structure is formed, the stress-strain curve is essentially representative of parallel tensile tests and ϵ_{max} at least, should be rather insensitive to the initial geometry.

The stiffness of the experimental apparatus will also play a role in the deformation processes of the adhesive film during debonding. In probe tests, the stiffness of the apparatus is usually much larger than the stiffness of the film. However in a peel test this is no longer true and it is well known that significantly different results can be obtained with different backings. This will also hold in probe tests if a tack test is performed on a PSA on its backing. If the backing is soft and elastic it will act as an additional reservoir of elastic energy while if it is viscoelastic, it will strongly alter the rate and contact time dependence of the tack test of the adhesive. Therefore probe tests of adhesives should, whenever possible, be conducted without a backing.

Finally, the notion of confinement also applies to peel tests; in this case the confinement level may be given by the ratio between the width of the tape and the thickness of the film. Since this ratio is usually large, results on peel tests should be correlated with flat probe tests but experimental confirmation of this statement is presently not available in the literature.

VI. SURFACE EFFECTS

PSA are normally designed to stick to most surfaces and to be therefore rather insensitive to the nature of the surface of the adherent. This is why, in the previous sections, we have considered mainly the rheological properties of the adhesive rather than the interfacial chemistry. However based on the theoretical arguments set forth in section III, there are two major causes of poor adhesion of a PSA to a surface: low G_c and poor contact.

The first case is related to the arguments given in section VI.1: if the interfacial G_c (static but also dynamic) is too low, once cavities are nucleated at the interface, they can easily propagate, coalesce and debonding occurs without any fibril formation. The second case is discussed in section VI.2 and occurs when the elastic modulus of the PSA is too high (Dahlquist's criterion is not met) or when the surface is too rough for the adhesive to conform to it during the short contact time.

Before we proceed, a word of caution is necessary here in terms of our use of the parameter G_c . In fracture mechanics, G_c has the meaning of an energy per unit area necessary for a crack to advance. For elastic elastomers, G_c is a unique function of the velocity of the advancing crack and can be determined with a fracture mechanics test such as the JKR test²⁵. Unfortunately, the independent determination of G_c by the same method is very difficult for viscoelastic materials^{66,67} since it will depend on the history-dependent degree of relaxation of the adhesive. However as a phenomenological parameter associated with the amount of energy dissipated by the advance of a crack front (per unit area), it can be very useful and simplify the description of the mechanisms.

VI.1. Adhesion on low G_c surfaces

Several studies have been undertaken to investigate the adhesion of model PSA on low energy surfaces or more generally on low G_c surface^{7,68}. Examples of such surfaces are silicone rubbers, commonly used for release coatings, polyethylene,

polypropylene and polycarbamates. These early results were somewhat contradictory and did not provide any explanation of the observed dependence on surface tension. Generally, tack decreased markedly when the surface energy of the adherent decreased well below that of the adhesive. More recently peel experiments showed that for soft adhesives, it is not necessarily the surface tension of the adherent which is the controlling parameter but rather the resistance to shear of the interface⁶⁹. The cause for this effect, at the molecular level, remains however a controversial issue so we will focus here on a more macroscopic description of the tack experiment of a PSA on a low G_c surface. This description should be kept in mind when interpreting experimental data obtained on such surfaces.

The essential difference between a low energy surface and a high energy surface can be visualized through the comparative analysis of probe tack tests and has been recently discussed⁴¹. For a given experimental geometry, the key parameter controlling the behavior of the adhesive is the ratio of the energy release rate over the modulus G_c/E . Three different cases can be observed as a function of G_c/E :

For high G_c/E , the initial mechanism of failure is cavitation and fibrillation. The maximum extension of the fibrils is not controlled by the surface but by the rheological behavior of the adhesive in elongation. This is the standard case for a PSA on steel or glass.

For intermediate values of G_c/E , the initial failure mechanism can still be cavitation but the maximum extension of the fibrils is controlled by the surface. An example of this situation is given on figure 21: the measured σ_{max} is identical for both surfaces but ϵ_{max} is very different. A more detailed analysis of the debonding mechanisms reveals that the initiation of failure occurs at about the same level of stress, but the lateral propagation of the existing defects is much faster for the low G_c situation. If this lateral propagation is fast enough, it prevents any growth of cavities in the bulk of the adhesive and therefore the formation of the elongated foam of bridging fibrils. What happens is rather a coalescence of adjoining cracks and global debonding of the adhesive film from the probe at relatively low levels of deformation.

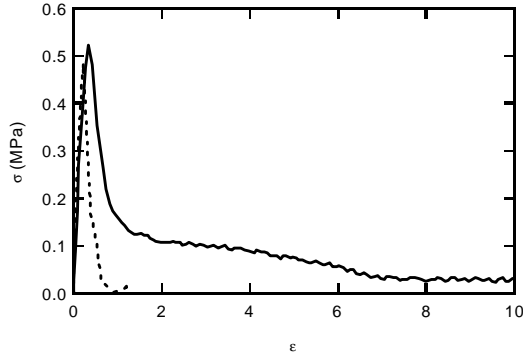


Figure 21: Stress-strain curves of a soft adhesive (high and intermediate G_c/E) on steel (solid line) and for a low G_c surface-adherent pair (dashed line). $V_{deb} = 100 \mu\text{m/s}$. Data from ⁴¹.

Finally for very low values of G_c/E , the initiation mechanism is no longer cavitation but internal crack propagation. This can occur at lower levels of stress so that both σ_{max} and ϵ_{max} are significantly decreased. An example of that situation is given on figure 22. This very different initiation mechanism is also clearly apparent from the video images of the debonding process shown on figure 22b.

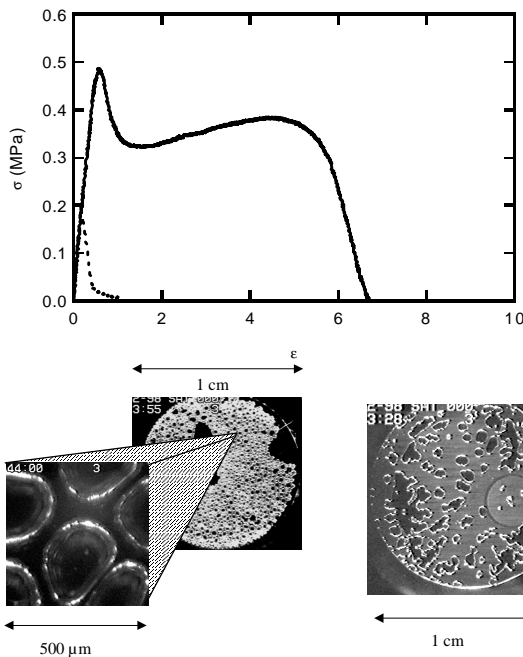


Figure 22: a) Stress-strain curves of the same hard elastic adhesive on steel (solid line) and on a low G_c surface-adherent pair (dashed line). b) Video captures of the debonding process for both surfaces. $V_{deb} = 1 \mu\text{m/s}$. Note the relatively small cavities observed for the steel surface and the large irregularly shaped interfacial cracks observed for the low energy surface. Data from ⁴¹.

This description is simple and yet very general. It can explain why transitions from interfacial

separation to fibrillation are observed by changing V_{deb} , the surface roughness or surface chemistry or the contact time. In each one of these cases, the change in the experimental parameter had an effect both on E and on G_c . However the magnitude of this effect is generally very different and sometimes in opposite directions resulting in a very large change in G_c/E .

VI.2. Effect of surface roughness

The effect of surface roughness is in many ways much more complicated, and it is impossible at present to give trends generally valid for all PSA-surface pairs. It has been discussed theoretically first for perfectly elastic systems⁷⁰ and then for more viscoelastic systems¹⁵. Experiments have shown consistently that for PSA (unlike for other types of adhesives) the presence of a high level of surface roughness was detrimental for adhesion.

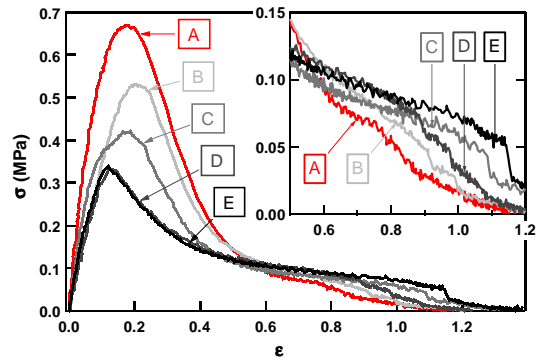


Figure 23: Stress-strain curves of an acrylic PSA on rough surfaces with a different average amplitude R_a of the roughness but with the same wavelength. A : $R_a = 11 \text{ nm}$; B : $R_a = 23 \text{ nm}$; C : $R_a = 46 \text{ nm}$; D : $R_a = 114 \text{ nm}$; E : $R_a = 148 \text{ nm}$. $V_{deb} = 30 \mu\text{m/s}$; $T = 20 \text{ }^\circ\text{C}$. Data from ⁷¹.

This, it was argued, was due to the limitation of the real surface of contact due to the asperities^{14,15}. As discussed briefly in section III.1, when an elastic layer is brought in contact with a rough hard surface, it tries to comply to the topography of the surface, but if the balance between the amplitude of the roughness and the elastic modulus does not comply to equation 1, contact may be incomplete. This first simplistic picture is however inconsistent with the experimental observation that even for low modulus PSA, an effect of surface roughness is observed. This effect is however magnified when the PSA has a relatively high elastic modulus. A more realistic view may be that the presence of a surface roughness creates an inhomogeneous strain field around the surface and creates therefore

pockets of residual tensile stress which will become preferential nucleation sites for cavities. Recent more systematic experiments⁷¹ have shown that the amplitude of the surface roughness had a direct effect on the level of stress at which the cavities appeared as shown on figure 23.

On the other hand, experiments with triblock based adhesives have shown that if nucleation is not affected, (for example at high temperature), the propagation of the cracks can be greatly affected by the roughness⁶⁵. In this regime, as shown on figure 24, σ_{max} is hardly affected but the fibril formation can be completely suppressed on smooth surfaces, by a rapid lateral propagation of nucleating cavities in an analogous way as what is observed for the intermediate G_c/E case discussed in the preceding section.

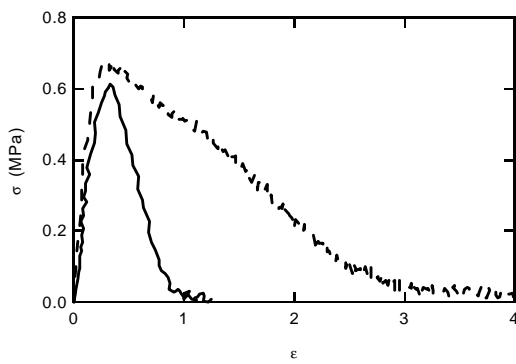


Figure 24: Stress-strain curves for an SIS + 50 wt % resin adhesive on a rough (dashed line) and on a smooth (solid line) steel surface⁴⁴. $T = 60^\circ\text{C}$; $V_{deb} = 100 \mu\text{m/s}$.

VII. CONCLUSIONS

In this chapter we have attempted to review, both the main material properties which are required for a PSA to be tacky and how experimental parameters affect the practical evaluation of tackiness. Although it must be clear from the previous sections that the bonding and debonding of a PSA from a surface is a complicated process, some important parameters have been identified: The elastic modulus E' obtained from small strain oscillatory rheological measurements in the linear viscoelastic regime.

The maximum extension of the adhesive in a tensile test ϵ_{max} or its elongational rheological properties. The spectrum of relaxation times of the adhesive.

E' should be in a window of 0.01 to 0.1 MPa. Above that level, proper bonding and fibril formation are reduced and below that level, viscoelastic dissipation during the debonding process will be too low. ϵ_{max} controls the maximum

extension of the fibrils and therefore plays a major role in the measured debonding energy. A relatively small ϵ_{max} is typically desirable for removable PSA while a larger value is often characteristic of semi-permanent ones. A reasonable idea of the value of ϵ_{max} can in principle be obtained by a characterization of the adhesive in elongational deformation.

Finally a broad spectrum of relaxation times is necessary to ensure both quick bonding (short relaxation times) and reasonable fibril stability (long relaxation times) as well as to impart a broad temperature window of use.

Additionally to these important material parameters of the PSA, the surface can also play a role in controlling tackiness in certain cases. Rough surfaces can prevent proper bonding and, by forming defects, initiate failure during debonding, both effects reducing tack. Low energy surfaces can also influence tack by preventing fibril formation and the relevant parameter to predict whether this will occur or not is the ratio of the critical energy release rate G_c over the elastic modulus E .

VIII. FURTHER READING

Hammond, F. H. (1989). Tack. Handbook of pressure sensitive adhesive technology. D. Satas. New York, Van Nostrand Reinhold. **1**: 38-60.

Zosel, A. (1992). "Fracture energy and tack of pressure sensitive adhesives." Advances in Pressure Sensitive Adhesive Technology **1**: 92-127.

Creton, C. (1997). Materials Science of Pressure-Sensitive-Adhesives. Processing of Polymers. H. E. H. Meijer. Weinheim, VCH. **18**: 707-741.

Gay, C. and L. Leibler (1999). "On Stickiness." Physics Today: 47-52.

IX. REFERENCES

- (1) Chang, E. P. *J. Adhes.* **1991**, *34*, 189-200.
- (2) Chang, E. P. *J. Adhes.* **1997**, *60*, 233-248.
- (3) Tse, M. F.; Jacob, L. *J. Adhes.* **1996**, *56*, 79-95.
- (4) Zosel, A. *J. Adhes.* **1989**, *30*, 135-149.
- (5) Urahama, Y. *J. Adhes.* **1989**, *31*, 47-58.
- (6) Hammond, F. H. *ASTM Spec. Tech. Publ.* **1964**, *360*, 123-134.
- (7) Zosel, A. *Colloid Polym. Sci.* **1985**, *263*, 541-553.
- (8) Lakrout, H.; Sergot, P.; Creton, C. *J. Adhes.* **1999**, *69*, 307-359.
- (9) Tordjeman, P.; Papon, E.; Villenave, J.-J. *J. Polym. Sci. B Polym. Phys.* **2000**, *38*, 1201-1208.
- (10) Chuang, H. K.; Chiu, C.; Paniagua, R. *Adh. Age* **1997**, 18-23.
- (11) Crosby, A. J.; Shull, K. R. *J. Polym. Sci. B Polym. Phys.* **1999**, *37*, 3455-3472.
- (12) Lakrout, H., PhD. Thesis, Université Paris 7, 1998
- (13) Dahlquist, C. A. *Pressure-Sensitive adhesives*; Patrick, R. L., Ed.; Dekker, 1969; Vol. 2, pp 219-260.
- (14) Creton, C.; Leibler, L. *J. Polym. Sci. B Polym. Phys.* **1996**, *34*, 545-554.
- (15) Hui, C. Y.; Lin, Y. Y.; Baney, J. M. *J. Polym. Sci. B Polym. Phys.* **2000**, *38*, 1485-1495.
- (16) Gay, C.; Leibler, L. *Phys. Rev. Lett.* **1999**, *82*, 936-939.
- (17) Gay, C.; Leibler, L. *Physics Today* **1999**, 47-52.
- (18) Lakrout, H.; Creton, C.; Ahn, D.; Shull, K. R., submitted to *Macromolecules*
- (19) Gent, A. N.; Lindley, P. B. *Proc. Roy. Soc. London, A* **1958**, *249 A*, 195-205.
- (20) Williams, M. L.; Schapery, R. A. *Int. J. Fract. Mech.* **1965**, *1*, 64-71.
- (21) Chikina, I.; Gay, C. *Phys. Rev. Lett.* **2000**, *85*, 4546-4549.
- (22) Lin, Y. Y.; Hui, C. Y.; Conway, H. D. *J. Polym. Sci. B Polym. Phys.* **2000**, *38*, 2769-2784.
- (23) Creton, C.; Lakrout, H. *J. Polym. Sci. B Polym. Phys.* **2000**, *38*, 965-979.
- (24) Gent, A. N.; Schultz, J. *J. Adhes.* **1972**, *3*, 281-294.
- (25) Maugis, D.; Barquins, M. *J. Phys. D: Appl. Phys.* **1978**, *11*, 1989-2023.
- (26) Barquins, M.; Maugis, D. *J. Adhes.* **1981**, *13*, 53-65.
- (27) Creton, C. *Materials Science of Pressure-Sensitive-Adhesives*; 1st ed.; Meijer, H. E. H., Ed.; VCH: Weinheim, 1997; Vol. 18, pp 707-741.
- (28) Good, R. J.; Gupta, R. K. *J. Adhes.* **1988**, *26*, 13-36.
- (29) Baljon, A. R. C.; Robbins, M. O. *Science* **1996**, *271*, 482-483.
- (30) McKinley, G. H.; Hassager, O. *J. Rheol.* **1999**, *43*, 1195-1212.
- (31) Gersappe, D.; Robbins, M. O. *Europhys. Lett.* **1999**, *48*, 150-155.
- (32) Crosby, A. J.; Shull, K. R.; Lakrout, H.; Creton, C. *J. Appl. Phys.* **2000**, *88*, 2956-2966.
- (33) Ferry, J. D. *Viscoelastic Properties of Polymers*; 3rd ed.; Wiley, 1980; Vol. 1.
- (34) Doi, M.; Edwards, S. F. *The theory of polymer dynamics*; Oxford, 1986.
- (35) Zosel, A. *Adv. Pressure Sensitive Adhes. Technol.* **1992**, *1*, 92-127.
- (36) Ahn, D.; Shull, K. R. *Langmuir* **1998**, *14*, 3637-3645.
- (37) Aubrey, D. W.; Ginosatis, S. *J. Adhes.* **1981**, *12*, 189-198.
- (38) Chan, H.; Howard, G. J. *J. Adhes.* **1978**, *9*, 279-301.
- (39) Kreneski, M. A.; Johnson, J. F. *Polym. Eng. Sci.* **1989**, *29*, 36-43.
- (40) Zosel, A. *Int. J. Adhes. Adh.* **1998**, *18*, 265-271.
- (41) Creton, C.; Hooker, J. C.; Shull, K. R., *Langmuir* in press
- (42) Zosel, A. *J. Adhes.* **1991**, *34*, 201-209.
- (43) Webster, I. *Int. J. Adhes. Adh.* **1999**, *19*, 29-34.
- (44) Hooker, J. C.; Creton, C. **2000**.
- (45) Flanigan, C. M.; Crosby, A. J.; Shull, K. R. *Macromolecules* **1999**, *32*, 7251-7262.
- (46) Komatsuzaki, S. *Tappi Hot Melt Symposium* **1999**, 171-178.
- (47) Spence, B. A.; Higgins, J. W. *Journal of Adhesion Sealant Council* **1997**, 237-255.
- (48) de Crevoisier, G.; Fabre, P.; Corpart, J.-M.; Leibler, L. *Science* **1999**, *285*, 1246-1249.
- (49) Aymonier-Marçais, A.; Papon, E.; Villenave, J. J.; Tordjeman, P.; Pirri, R.; Gérard, P., Proceedings of Euradh 2000; Lyon; 2000, pp 170-175.
- (50) Portigliatti, M.; Hervet, H.; Léger, L. *C.R. Acad. Sci. Paris, IV* **2000**, *1*, 1187-1196.

- (51) Aubrey, D. W.; Sherriff, M. *Journal of Polymer Science, Polymer Chemistry Edition* **1978**, *16*, 2631-2643.
- (52) Aubrey, D. W.; Sherriff, M. *Journal of Polymer Science, Polymer Chemistry Edition* **1980**, *18*, 2597-2608.
- (53) Class, J. B.; Chu, S. G. *J. Appl. Polym. Sci.* **1985**, *30*, 805-814.
- (54) Class, J. B.; Chu, S. G. *J. Appl. Polym. Sci.* **1985**, *30*, 825-842.
- (55) Class, J. B.; Chu, S. G. *J. Appl. Polym. Sci.* **1985**, *30*, 815-824.
- (56) Kim, H. J.; Mizumachi, H. *J. Adhes.* **1995**, *49*, 113-132.
- (57) Tancrede, J. M. *Journal of Adhesion Sealant Council* **1998**, (Spring), 13-27.
- (58) Satas, D. *Handbook of Pressure Sensitive Adhesive Technology*; 2nd ed.; Satas, D., Ed.; Van Nostrand Reinhold: New York, 1989; Vol. 1, pp 940.
- (59) Zosel, A.; Schuler, B. *J. Adhes.* **1999**, *70*, 179-195.
- (60) Delgado, J.; Kinning, D. J.; Lu, Y. Y.; Tran, T. V., Proceedings of 19th Annual conference of the Adhesion Society; 1996, pp 342-345.
- (61) Gent, A. N.; Petrich, R. P. *Proc. Roy. Soc. London, A* **1969**, *310*, 433-448.
- (62) Benyahia, L.; Verdier, C.; Piau, J. M. *J. Adhes.* **1997**, *62*, 45-73.
- (63) Ondarçuhu, T. *J. Phys. II* **1997**, *7*, 1893-1916.
- (64) Zosel, A. *J. Adhesion Sci. Tech.* **1997**, *11*, 1447-1457.
- (65) Hooker, J. C.; Creton, C.; Tordjeman, P.; Shull, K. R., Proceedings of 22nd Annual Meeting of the Adhesion Society; Panama City; 1999, pp 415-417.
- (66) Lin, Y. Y.; Hui, C. Y.; Baney, J. M. *J. Phys. D: Appl. Phys.* **1999**, *32*, 2250-2260.
- (67) Baney J.M.; C.Y., H. *J. Appl. Phys.* **1999**, *86*, 4232-4241.
- (68) Toyama, M.; Ito, T.; Nukatsuka, H.; Ikeda, M. *Journal of Applied Polymer Science* **1973**, *17*, 3495-3502.
- (69) Zhang Newby, B.-M.; Chaudhury, M. K.; Brown, H. R. *Science* **1995**, *269*, 1407-1409.
- (70) Fuller, K. N. G.; Tabor, D. *Proc. Roy. Soc. London, A* **1975**, *A345*, 327-342.
- (71) Chiche, A.; Pareige, P.; Creton, C. *C.R. Acad. Sci. Paris, IV* **2000**, *1*, 1197-1204.